LETTER

Efficiency of energy harvesting out of colored Lévy fluctuations by a harmonic oscillator with piezoelectric transducer

To cite this article: M. E. Giuliano *et al* 2023 *EPL* **144** 11006

A Letters Journal Exploring the Frontiers of Physics

October 2023

EPL, **144** (2023) 11006
doi: 10.1209/0295-5075/acfdca

www.epljournal.org

Efficiency of energy harvesting out of colored Lévy fluctuations by a harmonic oscillator with piezoelectric transducer

M. E. Giuliano[(a)], A. D. Sánchez, B. Combi and R. R. Deza

IFIMAR (UNMdP & CONICET), Faculty of Exact & Natural Sciences, National University of Mar del Plata (UNMdP) - Funes 3350, B7602AYL, Mar del Plata, Argentina

received 27 February 2023; accepted in final form 27 September 2023
published online 16 October 2023

Abstract – The efficiency of a linear kinetic energy harvester by piezoelectric transduction —when driven by colored α-stable Lévy noise— is the focus of this study. Analytical results are obtained for the harvested power (in the adiabatic approximation $\ddot{x} \cong 0$ and for very large load circuit's time constant τ_p), which are accurately validated by numerical simulations. In addition, an analytical expression is obtained for the characteristic time the system takes to reach a stationary regime; this information is crucial to calculate averaged quantities through simulations, given the large dispersion between realizations due to the infinite variance of the Lévy noise.

Introduction. – Ever since the dawn of the transistor era, batteries have reigned in the kingdom of small-power electronics. Today —whereas on one hand climate change and air pollution spur the replacement of fuel engines in cars— the decisive downscaling toward micro- and even nano-devices (as well as the spread of embedded and remote solutions) on the other, urge to feed small-power circuits otherwise, so making them lighter and more reliable. The goal of harvesting energy from the environment has captured the interest of researchers for many years. Various types of harvesters and applications have been studied [1–3]. A type that is widely studied due to its great transduction capacity is piezoelectric harvesting of kinetic energy [4–11]. This type of harvester can be modeled as a test mass subject to a (linear or nonlinear) spring, whose elongation is linearly transduced into an output voltage. The mass is forced by environmental vibrations (hereafter referred to as "noise" since they can be usually regarded as random) [2,12]. Since early studies aimed at energy harvesting from sea waves, they considered linear harmonic oscillators subject to sinusoidal noises (resonant energy harvesting). However, environmental vibrations are rarely monochromatic (*i.e.*, have their spectrum peaked around a dominant frequency). Rather the opposite occurs: they have their frequencies distributed over a wide enough bandwidth, causing the performance of resonant energy harvesters to drop considerably. To counteract this inconvenience, nonlinear oscillators have been proposed as an alternative [13–17]. However, for Gaussian white noise (which is the typical representation of noises with finite variance and wide enough bandwidth), it has been shown that nonlinear oscillators do not outperform by much the linear ones [13–15]. For narrower (but still wide) bandwidth —what is known as "colored noise"— mono- or bistable nonlinear oscillators can under certain circumstances present an advantage over linear ones [16,17].

Strictly speaking, white noise is an unphysical abstraction. Any physical source will produce colored noise of wider or narrower bandwidth [13]. As far as the noise variance is finite —it fulfills the Central Limit Theorem (CLT)— and its self-correlation function decays faster than a power of time, it can be modeled as an Ornstein-Uhlenbeck (OU) one (namely Gaussian, exponentially correlated noise[1]).

Recall however that the CLT is a consequence of the Gaussian distribution being *stable* under the addition of independent stochastic variables. Lévy [18] found the conditions for stochastic variables with infinite variance (and still wilder ones) to keep this property. Noises of this kind *do* exist in nature: The general class of non-Gaussian processes known as α-stable Lévy noise ($0 < \alpha \leq 2$ being known as the *stability parameter*, with $\alpha = 2$ corresponding to Gaussian noise) describes with naturalness *complex* environments (those in which scale separation is not feasible, due to their strong interaction) [19–23]. These processes, featuring a power-law distribution of

[(a)]E-mail: mgiuliano@mdp.edu.ar (corresponding author)

[1]Complex sources may produce colored noises whose spectrum decays more slowly (f^{α}-noise).

jump lengths, are qualitatively grouped into *Lévy walks* (for $\alpha \sim 2$) and *Lévy flights* (for $\alpha \ll 2$). These noises have been found suitable to study thermoacoustic instabilities (which can have catastrophic consequences) in high-performance combustion systems [24], as well as complex dynamics of a conceptual airfoil structure [25]. Many studies in the biological field include this type of noise [26–29], featuring, *e.g.*, noise-induced chimera states (here meaning coexistence of coherence and incoherence) in a small-world Hindmarsh-Rose neuronal network [28]. Also, the heartbeat has been seen to be well modeled using the Lévy process [30,31], and heart-mounted piezoelectric sensors are being studied to power pacemakers [32–34] since as shown in [35,36], this type of noise improves the performance of piezoelectric harvesters (the more frequent occurrence of large jumps in Lévy noises translates into a larger r.m.s. voltage). Other recent works considering Lévy noises are [37–39].

After characterizing the vibration harvester model and the α-stable Lévy noise, we perform a thorough check for $\alpha = 2$ against the results in [10] and then present performance measures for α ranging between 1.5 and 2.

Vibration harvester model. – A simple case of a mechanical vibration harvester is the one-degree-of-freedom damped harmonic oscillator, forced by random mechanical vibrations from external sources and coupled to a mechanical-electrical transducer [2,10–12],

$$\begin{aligned} \ddot{x}(t) &= -b\,\dot{x}(t) - k_V\,V(t) - \omega_0^2\,x(t) + \xi(t), \\ \dot{V}(t) &= k_c\,\dot{x}(t) - \frac{V(t)}{\tau_p}. \end{aligned} \tag{1}$$

Here x represents the displacement from equilibrium position of the oscillator, $\dot{x}$ its velocity and $\ddot{x}$ its acceleration. The electric potential V is generated by the transducer (here of piezoelectric nature). Parameter b represents friction with the surrounding environment. This system has capacitance C and is coupled to a load resistance R_L, yielding a load circuit time constant $\tau_p = R_L C$. Parameters k_c and k_V are electromechanical coupling coefficients and ω_0 is the characteristic frequency of the free oscillator. The second-order differential system of equations (1) can be converted into a first-order one:

$$\begin{aligned} \dot{x}(t) &= v(t), \\ \dot{v}(t) &= -b\,v(t) - k_V\,V(t) - \omega_0^2\,x(t) + \xi(t), \\ \dot{V}(t) &= k_c\,v(t) - \frac{V(t)}{\tau_p}. \end{aligned} \tag{2}$$

Observing that the third of eqs. (2) acts as a low-pass filter (so that the smaller the load characteristic decay rate $\omega_p = 1/\tau_p$, the more closely voltage V "follows" the excursions of x), an approximation that somewhat simplifies the system is to take $V(t) \cong k_c\,x(t)$ [16], wherefrom the average electrical power can be approximated by

$$P_R = \frac{V_{\rm rms}^2}{R_L} \cong \frac{k_c^2}{R_L}\,x_{\rm rms}^2. \tag{3}$$

However, this improvement in the tracking of $V_{\rm rms}$ to $x_{\rm rms}$ by taking τ_p much larger than the other characteristic times of the system, has a cost: P_R becomes depressed by the large factor R_L.

α-stable Lévy noise. – Throughout this work, we regard the external forcing $\xi(t)$ in the second of eqs. (2) as a symmetric Ornstein-Uhlenbeck-Lévy process (OULP) with α-stable distribution, *noise amplitude* $\sigma > 0$, and *inverse characteristic correlation time* $\lambda = \tau^{-1}$. The OULP can be generated through a Langevin equation of the form

$$\dot{\xi}(t) = -\lambda\,\xi(t) + \sigma\,\eta(t), \tag{4}$$

from a symmetric and δ-correlated Lévy noise η [19,20]. Process η (determined by its *stability parameter* α) is defined by its characteristic function

$$\tilde{p}_{\sigma\eta}(k,t) = \tilde{p}_\eta(\sigma k, t) = \exp(-\sigma^\alpha |k|^\alpha t) \tag{5}$$

($\tilde{p}_\eta(k,t) = \exp(-|k|^\alpha t)$ if $\sigma = 1$). From eqs. (4), (5), the characteristic function of an OULP is thus [22]

$$\tilde{p}_\xi(k,t) = \exp\left[-\frac{\sigma^\alpha}{\alpha\lambda}\,|k|^\alpha\,(1 - e^{-\alpha\lambda t})\right]. \tag{6}$$

Defining[2] a noise intensity $D > 0$ by means of $\sigma := \lambda D^{1/\alpha}$ and taking $\alpha = 2$, Gaussian OU noise is recovered, with correlation function

$$C(u) = \langle \xi(t)\xi(t+u)\rangle = D\,\lambda\,e^{-\lambda|u|}. \tag{7}$$

Here $\langle\cdot\rangle$ stands for mathematical expectation. As $\lambda \to \infty$, $C(u) \to D\,\delta(u)$, and ξ becomes a δ-correlated noise.

The most remarkable feature of Lévy processes is that they have infinite variance when $0 < \alpha < 2$ (and infinite mean if $0 < \alpha < 1$). From eq. (6) we see that the OULP reaches steady state

$$\tilde{p}_\xi^{\rm st}(k) = \exp\left(-\frac{\sigma^\alpha}{\alpha\lambda}\,|k|^\alpha\right)$$

for α and λ fixed, whenever $t \gg (\alpha\lambda)^{-1}$. Since

$$\langle \xi^n \rangle_{\rm st} = (-i)^n\,\left.\frac{{\rm d}^n \tilde{p}_\xi^{\rm st}(k)}{{\rm d}k^n}\right|_{k=0}, \tag{8}$$

it turns out that $\langle \xi^2 \rangle_{\rm st} = \infty$ for $0 < \alpha < 2$. This behavior can be hinted at when one sees a diagram of the trajectory of a Brownian particle subjected to Lévy noise [22]. The large difference in scale of the jumps causes the variance to blow up. However, these large excursions could in

[2]Had we defined $\sigma := (\lambda D)^{1/2}$, then $C(u) = D\,e^{-\lambda|u|}$. This correlation function was used in [10] to show that when a linear harmonic harvester is subjected to Gaussian colored noise with fixed amplitude D and correlation decay rate λ, the system (2) achieves resonance (of stochastic nature, but *not* stochastic resonance) when λ is close to the natural electromechanic frequency $\sqrt{\omega_0^2 + k_c k_V}$. We also recover eq. (7) if $D \propto \lambda$ and $\lambda \to \infty$.

principle be used to harvest more energy by piezoelectric transduction. According to eq. (3), once τ_p is set large enough (depending on the system) and there is good synchronization between V and x, the only way to increase P_R is by increasing $x_{\rm rms}^2$ as much as possible, and that is where Lévy processes come in.

Analytical results. – Using the techniques of refs. [19–22], one can think of obtaining an approximate solution of the characteristic function $\tilde{p}_x(k,t)$, and then using $V(t) \cong k_c\, x(t)$. To that end, τ_p is taken to be much larger than the other characteristic times of the system. From eqs. (1) and (4),

$$\begin{aligned} \ddot{x}(t) &\cong -b\,\dot{x}(t) - (k_V\, k_c + \omega_0^2)\, x(t) + \xi(t), \\ \dot{\xi}(t) &= -\lambda\, \xi(t) + \sigma\, \eta(t). \end{aligned}$$

Using the adiabatic approximation $\ddot{x} \cong 0$, we obtain

$$\begin{aligned} \dot{x}(t) \cong \dot{x}_a(t) = &-\frac{\lambda\,(k_V\, k_c + \omega_0^2)}{\lambda\, b + k_V\, k_c + \omega_0^2}\, x_a(t) \\ &+ \frac{\sigma}{\lambda\, b + k_V\, k_c + \omega_0^2}\, \eta(t). \end{aligned}$$

Since this expression is similar in form to eq. (4), the characteristic function for $x_a(t)$ is

$$\tilde{p}_{x_a}(k,t) = \exp\left[-\sigma_a(t)\,|k|^\alpha\right], \tag{9}$$

with

$$\begin{aligned} \sigma_a(t) = &\frac{\sigma^\alpha\,(\lambda\, b + k_V\, k_c + \omega_0^2)^{1-\alpha}}{\alpha\lambda(k_V\, k_c + \omega_0^2)} \\ &\times \left[1 - \exp\left(-\frac{\alpha\lambda(k_V\, k_c + \omega_0^2)}{\lambda\, b + k_V\, k_c + \omega_0^2}\, t\right)\right]. \end{aligned} \tag{10}$$

This characteristic function can be thought as that of a free particle submitted to a white Lévy noise, eq. (5), evaluated at an *effective* time $t_{\rm eff}$:

$$\tilde{p}_{x_a}(k,t) = \tilde{p}_{\sigma\eta}(k, t_{\rm eff}) = \exp\left(-\sigma^\alpha\,|k|^\alpha\, t_{\rm eff}\right).$$

Of course, $t_{\rm eff}$ is a function of the time t measured in the laboratory,

$$\begin{aligned} t_{\rm eff} = &\frac{(\lambda\, b + k_V\, k_c + \omega_0^2)^{1-\alpha}}{\alpha\lambda(k_V\, k_c + \omega_0^2)} \\ &\times \left[1 - \exp\left(-\frac{\alpha\lambda(k_V\, k_c + \omega_0^2)}{\lambda\, b + k_V\, k_c + \omega_0^2}\, t\right)\right]. \end{aligned}$$

For a given set of parameters, $t_{\rm eff}$ attains steady state when the laboratory time t is large enough (depending on its factor in the exponential). This gives us a rough estimate of the laboratory time t required for the system to reach steady state.

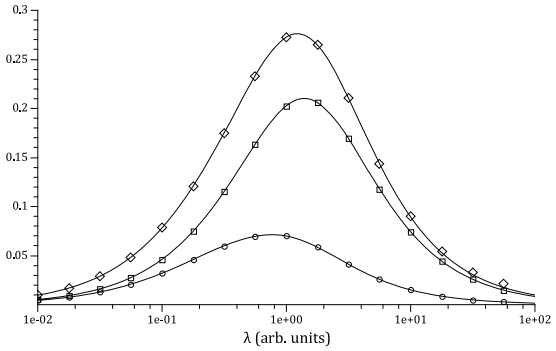

Fig. 1: Simulation results (in arbitrary units) for input noise power $P_{\rm in}$ ($\diamond$), mechanically dissipated power $P_{\rm diss}$ ($\square$), and power delivered to the load resistance P_R ($\circ$) —together with the theoretical curves from [10] (solid lines)— as functions of the noise correlation decay rate λ (log scale). Parameters $k_c = k_V = b = C = \omega_0 = D = 1$, $\tau_p = 2$, and $\alpha = 2$. The process was averaged over 10^3 realizations of noise and over time at steady state. The noise amplitude used is $\sigma = (\lambda D)^{1/\alpha}$.

Numerical results. – For the numerical simulation, symmetric white Lévy process was generated according to the proposal of ref. [23]. Then, stochastic second-order Runge-Kutta (Heun) integration of eq. (4) was used to generate the OULP and finally, the system in eqs. (2) —in the approximation of τ_p much larger than the other characteristic times of the system (we have adopted $\tau_p = 10^4$)— was integrated by the Heun method, to be able to reach large values of λ with confidence[3].

Check for $\alpha = 2$. In order to check that the symmetric white Lévy process generated according to the proposal of ref. [23] becomes Gaussian for $\alpha = 2$, we attempt to recover the results of [10] for OU noise. As seen in fig. 1, the simulation results (in arbitrary units) for the noise power input $P_{\rm in}$ to the system ($\diamond$), the power $P_{\rm diss}$ that is mechanically dissipated ($\square$), and the power P_R delivered to the load resistance ($\circ$) accurately follow the analytical results quoted in [10]. A resonance phenomenon of stochastic nature can be seen when λ is close to the natural electromechanic frequency $\sqrt{\omega_0^2 + k_c k_V}$.

Figure 2 compares P_R (filled markers) with $k_c^2 x_{\rm rms}^2 / R_L$ (empty markers) —both in log scale and as functions of λ (also in log scale)— for different values of τ_p. As the latter increases by an order of magnitude, both magnitudes become proportional (eq. (3)). Notice also the order-of-magnitude decrease of P_R as τ_p increases by an order of magnitude.

[3] In principle, for correlated enough noise there is no need to resort to stochastic integration. But nonetheless, it does no harm (it is just a matter of computational efficiency) and it becomes necessary for inverse correlation time $\lambda \to \infty$. Regarding the order of the stochastic Runge-Kutta algorithm, for stable systems it is again a matter of computational efficiency (a larger time step *vs.* the possibility of errors due to a cumbersome algorithm). Of course, we could have chosen a fourth-order stochastic Runge-Kutta algorithm, as in [26].

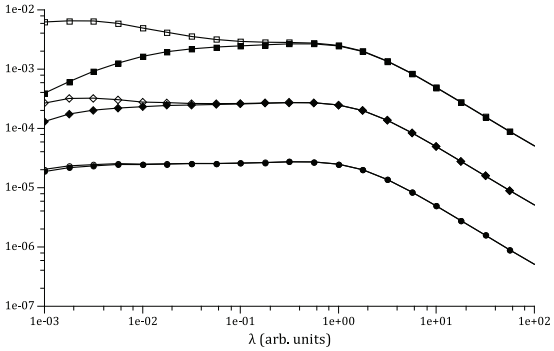

Fig. 2: Power delivered to the load resistance P_R (filled markers) and the amount $k_c^2 x_{\rm rms}^2/R_L$ (empty markers) as functions of the noise correlation decay rate λ, for different values of the load's characteristic time: $\tau_p = 10^2$ (□), $\tau_p = 10^3$ (◇), $\tau_p = 10^4$ (○). The solid lines were added only for better tracking of the markers. Same remaining parameters as in fig. 1.

Using eq. (8) on eqs. (9), (10) for $\tilde{p}_{x_a}(k,t)$, we get

$$x_{a,\rm rms}^2 = \langle x_a^2 \rangle = 2\,\sigma_a(t) = \frac{\sigma^2\,\left[1-\exp\left(-\frac{2\lambda(k_V\,k_c+\omega_0^2)}{\lambda\,b+k_V\,k_c+\omega_0^2}\,t\right)\right]}{\lambda\,(\lambda\,b+k_V\,k_c+\omega_0^2)(k_V\,k_c+\omega_0^2)}.$$

In order to reflect the results of [10] and [19], the white-noise approximation is resorted to. We choose $\sigma = \lambda(D)^{1/\alpha}$ ($\alpha = 2$), which yields

$$P_{a,R} = \frac{V_{a,\rm rms}^2}{R_L} = \frac{D\,\lambda\,k_c^2\,\left[1-\exp\left(-\frac{2\lambda(k_V\,k_c+\omega_0^2)}{\lambda\,b+k_V\,k_c+\omega_0^2}\,t\right)\right]}{R_L\,(\lambda\,b+k_V\,k_c+\omega_0^2)(k_V\,k_c+\omega_0^2)}. \quad (11)$$

In the steady state, eq. (11) reduces to

$$P_{a,R}^{\rm st} = \frac{D\,\lambda\,k_c^2}{R_L\,(\lambda\,b+k_V\,k_c+\omega_0^2)(k_V\,k_c+\omega_0^2)}. \quad (12)$$

Figure 3 compares the approximation in eq. (11) for the power P_R delivered to R_L (as a function of λ) with the full theoretical solution, eq. (5.4) in [10]. As expected, a large discrepancy takes place for λ close to ω_0. But also (as appreciated in the double-log-scale inset) when λ is small enough, due to the fact that the chosen laboratory time ($t = 1.5 \times 10^3$) becomes too short to reach the steady state (so the effect of the exponential is present). This approximation becomes exact for both $\lambda \to 0$ and $\lambda \to \infty$ [19], and agrees with the results of [10]. The upper dashed straight line indicates the limit $\lambda \to \infty$. The dot-dashed line in the inset corresponds to eq. (12), being indistinguishable of eq. (11) in the main plot.

Results for $\alpha < 2$. Even though the variance cannot be calculated, the theoretical curves $\sigma_a(t)$ are valid for any

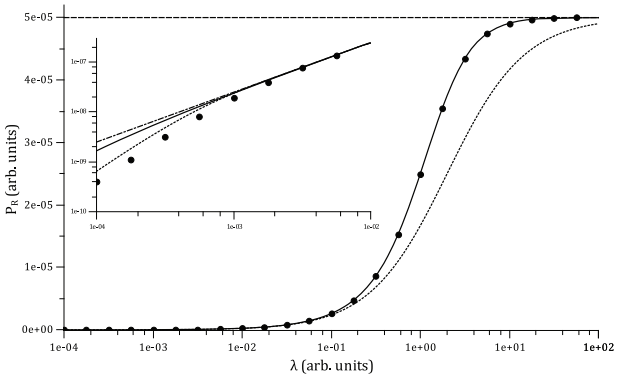

Fig. 3: $P_R(\lambda)$. Dotted curves correspond to eq. (11); dot-dashed ones (visible only in the inset) to eq. (12); solid curve, to eq. (5.4) in [10] (involving no approximation); discrete points, to the Heun numerical integration of system (2) and eq. (4); dashed upper straight line, to the white-noise limit. Load's time constant is $\tau_p = 10^4$ and lab time, $t = t_L$, given by (13). $\sigma = \lambda(D)^{1/2}$. The remaining values are indicated in fig. 1.

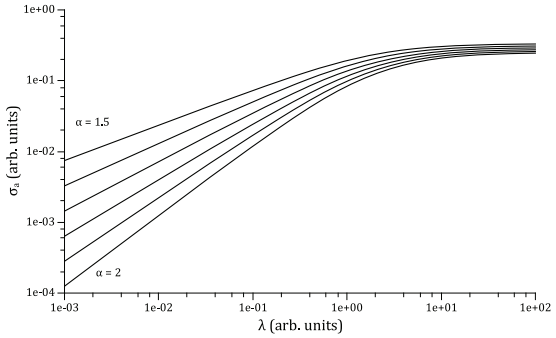

Fig. 4: From bottom to top, $\alpha = 2$, 1.9, 1.8, 1.7, 1.6, and 1.5. $\sigma_a(t = t_L)$ *vs.* λ (log-log scale). Remaining parameters as in fig. 1.

set of parameters. Figure 4 shows that —whereas for $\lambda > \omega_0$, the harvester is essentially driven by delta-correlated α-stable Lévy noise— a dramatic increase in $\sigma_a(t = t_L)$ takes place for $\lambda < \omega_0$ as α decreases from 2. The lab time, t_L, was chosen to make the argument in the exponential of (10) equal to 6 (a large enough value), *i.e.*,

$$t_L = 6\frac{\lambda\,b+k_V\,k_c+\omega_0^2}{\alpha\lambda(k_V\,k_c+\omega_0^2)}. \quad (13)$$

Figure 5 shows the numerical simulations of the harvested electrical power (as a function of λ) for different values of α. The consequences of divergent variance as the noise departs from Gaussian can be seen: The large-scale Lévy jumps make the curves rougher as α decreases from 2. However, the existence of a definite effective time shows the efficacy of the system's restoring force to generate stability. Notice the difference in scale as we move away from the Gaussian case. A fact to be stressed is that although the analytical variance is divergent, the extracted power is finite, and follows roughly the same behavior as $\sigma_a(t)$ in fig. 4.

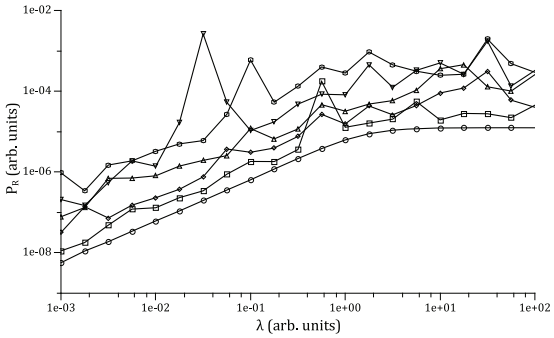

Fig. 5: From bottom to top, $\alpha = 2$ ($\circ$), 1.9 ($\square$), 1.8 ($\diamond$), 1.7 ($\triangle$), 1.6 ($\triangledown$), and 1.5 ($\bigcirc$). $V_{\rm rms}^2/R_L$ *vs.* noise correlation decay rate λ (log-log scale), from Heun integration (averaged over 10^3 realizations) of eqs. (2) and (4). Here $\tau_p = 10^4$, $t = t_L$, and $\sigma = \lambda(D)^{1/\alpha}$. Remaining parameters as in fig. 1.

Conclusions. – It was analytically and numerically confirmed that the Ornstein-Uhlenbeck process is indeed an exponentially correlated α-stable Lévy process, with $\alpha = 2$. The analytical and numerical results for the efficiency of the harvester —modeled as a damped linear harmonic oscillator, submitted to colored Lévy noises— confirm for $\alpha = 2$ the conclusions of [10] and [19]. As expected, Lévy flights greatly increase oscillator excursions, this being of great benefit to energy harvesting by piezoelectric transduction. Even though exhibiting differences with the numerical results, adiabatic approximations yield the same behavior. The latter are handy tools that can be used to improve the statistical averages in upcoming works. For example, finding the suitable time scale at which the system can be thought to have reached steady state, given the parameters of the harvester. In a companion work, we address the efficiency under symmetric OULP of nonlinear energy harvesters obeying shallow monostable potentials [35,36]. Also, the effect of asymmetric OULPs [40] will be studied.

* * *

The authors acknowledge support by UNMdP (through project EXA1033/21–15/E991) and by CONICET.

Data availability statement: All data that support the findings of this study are included within the article (and any supplementary files).

REFERENCES

[1] Priya S. and Inman D. J. (Editors), *Energy Harvesting Technologies* (Springer, New York, NY) 2009.
[2] Kaźmierski T. J. and Beeby S. (Editors), *Energy Harvesting Systems: Principles, Modeling and Applications* (Springer, New York, NY) 2011.
[3] Spreemann D. and Manoli Y., *Electromagnetic Vibration Energy Harvesting Devices: Architectures, Design, Modeling and Optimization* (Springer, Dordrecht) 2012.
[4] Beeby S. P., Tudor M. J. and White N. M., *Meas. Sci. Technol.*, **17** (2006) R175.
[5] Anton S. R. and Sodano H. A., *Smart Mater. Struct.*, **16** (2007) R1.
[6] Renno J. M., Daqaq M. F. and Inman D. J., *J. Sound Vib.*, **320** (2009) 386.
[7] Cammarano A., Burrow S. G., Barton D. A. W., Carrella A. and Clare L. R., *Smart Mater. Struct.*, **19** (2010) 055003.
[8] Kim H., Kim J.-H. and Kim J., *Int. J. Precis. Eng. Manuf.*, **12** (2011) 1129.
[9] Rey A. D., Servio P. and Herrera-Valencia E. E., *Phys. Rev. E*, **87** (2013) 022505.
[10] Méndez V., Campos D. and Horsthemke W., *Phys. Rev. E*, **88** (2013) 022124.
[11] Palau A. S., Méndez V., Campos D. and Horsthemke W., *Phys. Rev. E*, **91** (2015) 029904.
[12] Roundy S., Wright P. K. and Rabaey J. M. (Editors), *Energy Scavenging for Wireless Sensor Networks* (Springer, Boston, Mass.) 2004.
[13] Daqaq M. F., *J. Sound Vib.*, **330** (2011) 2554.
[14] Green P. L., Worden K., Atallah K. and Sims N. D., *J. Sound Vib.*, **331** (2012) 4504.
[15] Halvorsen E., *Phys. Rev. E*, **87** (2013) 042129.
[16] Gammaitoni L., Neri I. and Vocca H., *Appl. Phys. Lett.*, **94** (2009) 164102.
[17] Gammaitoni L., Neri I. and Vocca H., *Chem. Phys.*, **375** (2010) 435.
[18] Lévy P. P., *Théorie de l'Addition des Variables Aléatoires* (Gauthier-Villars, Paris) 1937.
[19] Srokowski T., *Acta Phys. Pol. B*, **42** (2011) 3.
[20] Dybiec B. and Gudowska-Nowak E., *Acta Phys. Pol. B*, **5** (2006) 37.
[21] Chechkin A. V., Gonchar V. Y., Klafter J., Metzler R. and Tanatarov L. V., *J. Stat. Phys.*, **115** (2004) 37.
[22] Jespersen S., Metzler R. and Fogedby H. C., *Phys. Rev. E*, **59** (1999) 2736.
[23] Weron A. and Weron R., in *Chaos—The Interplay Between Stochastic and Deterministic Behaviour*, edited by Garbaczewski P., Wolf M. and Weron A., *Lect. Notes Phys.*, Vol. **457** (Springer, Berlin) 1995.
[24] Zhang X., Xu Y., Liu Q., Kurths J. and Grebogi C., *Chaos*, **31** (2021) 113115.
[25] Liu Q., Xu Y. and Li Y., *Nonlinear Dyn.* (2023) 1.
[26] Wang Z., Xu Y. and Yang H., *Sci. China Technol. Sci.*, **59** (2016) 371.
[27] Xu Y., Li Y., Zhang H., Li X. and Kurths J., *Sci. Rep.*, **6** (2016) 31505.
[28] Wang Z., Xu Y., Li Y., Kapitaniak T. and Kurths J., *Chaos, Solitons Fractals*, **148** (2021) 110976.
[29] Wang Z., Li Y., Xu Y., Kapitaniak T. and Kurths J., *J. Stat. Mech.*, **2022** (2022) 053501.
[30] Peng C.-K. *et al.*, *Phys. Rev. Lett.*, **70** (1993) 1343.
[31] West B. J. and Turalska M., *Front. Physiol.*, **10** (2019) 1078.
[32] Karami M. A. and Inman D. J., *Appl. Phys. Lett.*, **100** (2012) 042901.
[33] Ansari M. H. and Karami M. A., *J. Phys.: Conf. Ser.*, **660** (2015) 012121.

[34] Li N. *et al.*, *ACS Nano*, **13** (2019) 2822.
[35] Deza J. I., Deza R. R. and Wio H. S., *EPL*, **100** (2012) 38001.
[36] Peña Rosselló J. I., Wio H. S., Deza R. R. and Hänggi P., *Eur. Phys. J. B*, **90** (2017) 1.
[37] Ma J. *et al.*, *Appl. Math. Mech.*, **42** (2021) 65.
[38] Zan W., Xu Y., Metzler R. and Kurths J., *J. Comput. Phys.*, **435** (2021) 110264.
[39] Zan W., Xu Y. and Kurths J., *Theor. Appl. Mech. Lett.*, **13** (2023) 100430.
[40] Li Y., Xu Y. and Kurths J., *Phys. Rev. E*, **96** (2017) 052121.